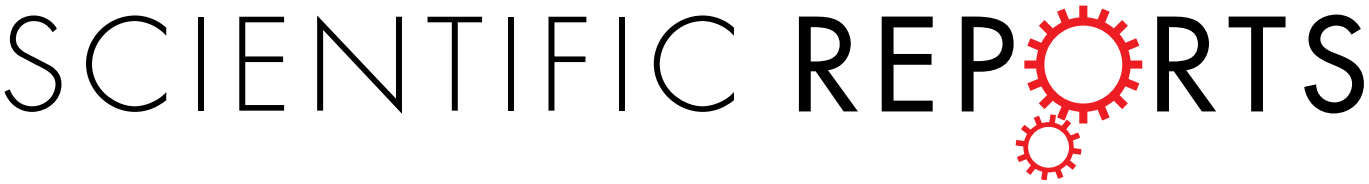

OPEN

Collective dynamics of identical phase oscillators with high-order coupling

Received: 27 April 2016
Accepted: 12 July 2016
Published: 05 August 2016

Can Xu[1,2,3], Hairong Xiang[2,3], Jian Gao[2,3] & Zhigang Zheng[1]

In this paper, we propose a framework to investigate the collective dynamics in ensembles of globally coupled phase oscillators when higher-order modes dominate the coupling. The spatiotemporal properties of the attractors in various regions of parameter space are analyzed. Furthermore, a detailed linear stability analysis proves that the stationary symmetric distribution is only neutrally stable in the marginal regime which stems from the generalized time-reversal symmetry. Moreover, the critical parameters of the transition among various regimes are determined analytically by both the Ott-Antonsen method and linear stability analysis, the transient dynamics are further revealed in terms of the characteristic curves method. Finally, for the more general initial condition the symmetric dynamics could be reduced to a rigorous three-dimensional manifold which shows that the neutrally stable chaos could also occur in this model for particular parameters. Our theoretical analysis and numerical results are consistent with each other, which can help us understand the dynamical properties in general systems with higher-order harmonics couplings.

Synchronization of coupled oscillators is an important issue in a wide variety of areas throughout the nature, and it has attracted much attention from the scientific community during the last decades[1]. Examples include the flashing of fireflies[2], electrochemical and spin-toque oscillators[3,4], pedestrians on footbridges[5], applauding person in a large audience[6] and others. Understanding the intrinsic dynamical properties of such system is therefore of considerable theoretical and experimental interest. Indeed, in the weak interaction limit, the dynamics of limit-cycle oscillators could be effectively described in terms of their phase variable θ. While the most famous case is the Kuramoto model[7], it stands out as the classical paradigm for studying the spontaneous emergence of collective synchronization in such system[8]. The form of phase equation obeys,

$$\dot{\theta}_i = \omega_i + \sum_{j=1}^{N} \Gamma(\theta_j - \theta_i), \tag{1}$$

where θ_i denotes the phase of the ith oscillator, ω_i is its natural frequency. $\Gamma(\theta)$ is 2π-periodic function representing the interaction between units. The simple choice of $\Gamma(\theta) = (K/N)\sin\theta$ leads to the classical Kuramoto model. Along the past decades the Kuramoto model with its generalizations have inspired and simulated a wealth of extensive studies because of both their simplicity for mathematical treatment and their relevance to practice[9–11]. In particular, when $\Gamma(\theta)$ includes higher harmonics, the system exhibits nontrivial dynamical features which have been reported in the recent works[12–15].

In many realistic systems, the higher-order harmonic term (especially the second) often plays an essential role in the interaction and even dominates the coupling function. Such as the Huygens pendulum system[16], the neuronal oscillators and genetic networks system[17], the globally coupled photochemical oscillators system[18], etc. In contrast to the pervious discussions of Kuramoto model containing higher order coupling, in the present work, we study phase equations of the following form,

[1]Institute of Systems Science and College of Information Science and Engineering, Huaqiao University, Xiamen 361021, China. [2]Department of Physics, Beijing Normal University, Beijing 100875, China. [3]Beijing-Hong Kong-Singapore Joint Center for Nonlinear and Complex Systems (Beijing), Beijing Normal University, Beijing 100875, China. Correspondence and requests for materials should be addressed to Z.Z. (email: zgzheng@hqu.edu.cn)

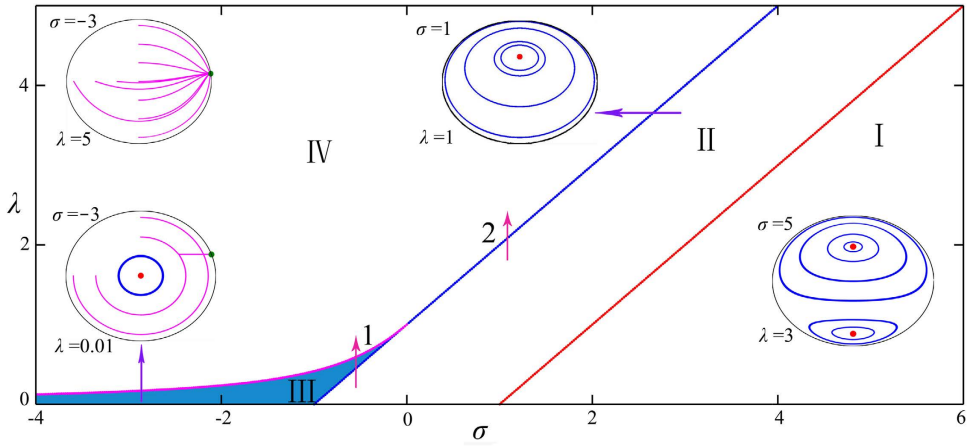

Figure 1. Phase diagram of the symmetric dynamics in the parameter space σ and λ. I is the double center regime, II is the single center regime, III is the center-synchrony coexistence regime, IV is the synchrony regime, respectively. The boundary curves are $\lambda = \sigma - \omega$ from I to II, $\lambda = \sigma + \omega$ from II to III or IV, $\lambda = \sigma + \sqrt{\omega^2 + \sigma^2}$ from III to IV, in the numerical simulations we set $\omega = 1$.

$$\dot{\theta}_i = \omega - \lambda \sin 2\theta_i + \frac{\sigma}{N}\sum_{j=1}^{N} \sin 2\theta_j, \quad i = 1, \cdots, N, \tag{2}$$

where ω is the frequency of identical oscillators, λ and σ are the global coupling strengths respectively. There are various motivations for the study of the current model. For example, in the Josephson junction arrays[19,20], the dynamics of a single element is determined by a double well potential and therefore the strong effects caused by the second harmonics is important. Another example is the star-like model with a central element and N leaves, where the case of single harmonic coupling was considered in the paper[21–29]. Similar to the mean-field coupling in the Kuramoto model, the interaction term in Eq. (2) turns out to be a driving force that does not depend on the phase of driven unit and is equally on every oscillator.

In this paper, we present a complete framework to investigate the collective dynamics of globally coupled phase oscillators when higher-order modes dominate the coupling function. It includes several aspects. First, we use the Ott-Antonsen method[30] to obtain the low-dimensional description of symmetric dynamics, and various states, such as the double-center, single-center, center-synchrony coexistence, and synchrony regimes, respectively are illustrated schematically in the phase diagram (Fig. 1). Furthermore, a detailed linear stability analysis based on the self-consistent approach is implemented and both the boundary curves between various steady states and eigenvalues of then are obtained analytically, which are consistent with the Ott-Antonsen method. Additionally, it has been proved that the linearized operator for the stationary symmetric distribution has infinitely many purely imaginary eigenvalues, which implies the stationary symmetric distribution is neutrally stable to perturbations in all the directions. Second, the two-cluster synchrony state is demonstrated which is initial-value dependent, and the general transient solutions of the distribution are calculated in term of the characteristics method. Finally, the general initial conditions for the phase oscillators which lie off the Poisson submanifold are considered, where the symmetric dynamics are governed by the three-dimensional Möbius transformation rigorously. Consequently, one can expect the chaotic behavior of both the symmetric dynamics r_2 and the degree of asymmetry r_1 to occur in the marginal regime. Extensive numerical simulations have been carried out to verify our theoretical analysis, in the following we report our main results both theoretically and numerically. These different aspects together present a global picture for the understanding of the dynamical properties in this system.

Results

Symmetric dynamics. We start by considering the high-order coupled phase oscillators model (2), without loss of generality, the range of the coupling strength is restricted to $\lambda > 0$ and $-\infty < \sigma < +\infty$ throughout the paper. The most important characteristic of the current model is the introduction of higher harmonics in the coupling function, and hence the generalized order parameters characterizing the collective behavior of the system[12] are needed, which yield,

$$r_n = R_n e^{i\Theta_n} = \frac{1}{N}\sum_{j=1}^{N} e^{in\theta_j}. \tag{3}$$

For $n \in$ integer, R_n is the magnitude of the complex, n-th order parameter, and Θ_n is its phase. As named in ref. 12, the amplitude R_2 measures the level of cluster synchrony, while R_1 measures the degree of asymmetry in clustering. Eq. (2) can be rewritten in terms of r_2 as

$$\dot{\theta}_i = \omega - \frac{\lambda}{2i}(e^{2i\theta_i} - e^{-2i\theta_i}) + \sigma \cdot \mathrm{Im}(r_2), \tag{4}$$

where Im represents the imaginary part. In the thermodynamic limit $N \to \infty$, Eq. (4) is equivalent to the continuity equation as a consequence of the conservation of the number of oscillators, i.e.,

$$\frac{\partial \rho}{\partial t} + \frac{\partial}{\partial \theta}\left\{\rho \cdot \left[\omega - \frac{\lambda}{2i}(e^{2i\theta} - e^{-2i\theta}) + \sigma \cdot \mathrm{Im}(r_2)\right]\right\} = 0. \tag{5}$$

Here $\rho(\theta, t)d\theta$ gives the fraction of oscillators which lie between θ and $\theta + d\theta$ at time t with the appropriate normalization condition $\int_0^{2\pi} \rho(\theta, t)d\theta = 1$. On its turn, the continuity limit of the generalized order parameters takes the form

$$r_n(t) = \int_0^{2\pi} e^{in\theta}\rho(\theta, t)d\theta. \tag{6}$$

Additionally, considering the 2π-periodicity of θ in the distribution function $\rho(\theta, t)$, which allows a Fourier expansion and can be written as

$$\rho(\theta, t) = \frac{1}{2\pi}\sum_{n=-\infty}^{\infty} r_n(t)e^{-in\theta} = \rho_s + \rho_a. \tag{7}$$

It is obvious that the n-th Fourier coefficient of $\rho(\theta, t)$ is just the n-th order parameter Eq. (6). Here ρ_s is the sum where n is even and symmetric in the sense that $\rho_s(\theta + \pi, t) = \rho_s(\theta, t)$, and ρ_a is the sum where n is odd which is antisymmetric with respect to the translation by π, $\rho_a(\theta + \pi, t) = -\rho_a(\theta, t)$. Then, substituting the expansion Eq. (7) into Eq. (5), we obtain two sets of equations as,

$$\dot{r}_{2n+1} = i(2n + 1)\left[\frac{i\lambda}{2} \cdot r_{2n+3} - \frac{i\lambda}{2}r_{2n-1} + (\omega + \sigma\ \mathrm{Im}(r_2)) \cdot r_{2n+1}\right], \tag{8}$$

for the odd Fourier coefficients, and

$$\dot{r}_{2n} = i(2n)\left[\frac{i\lambda}{2} \cdot r_{2n+2} - \frac{i\lambda}{2}r_{2n-2} + (\omega + \sigma\ \mathrm{Im}(r_2)) \cdot r_{2n}\right], \tag{9}$$

for the even Fourier coefficients. Eq. (8) together with Eq. (9) provide two sets of infinitely many coupled equations which evolve independently, for instance, the motion of r_2 is not only dependent on itself but also governed by r_4 and r_0. Going further, observing the specific form of Eqs (8) and (9), one notices that Eq. (8) has a trivial invariant manifold solution

$$r_n \equiv 0, \quad n \in odd, \tag{10}$$

and Eq. (9) has a non-trivial invariant manifold solution

$$r_{2n} \equiv r_2^n, \tag{11}$$

which is indeed the Ott-Antonsen ansatz[30,31]. The Ott-Antonsen method yields a special solution for the system provided that r_2 evolves according to a single ordinary differential equation(ODE) called the Riccati equation,

$$\dot{r}_2 = -\lambda r_2^2 + \lambda + 2i(\omega + \sigma\ \mathrm{Im}(r_2)) \cdot r_2, \tag{12}$$

and the solution of this kind turns out to form a two-dimensional invariant manifold, which is the set of Poisson kernels

$$\rho_s(2\theta, t) = \frac{1}{2\pi}\frac{1 - R_2^2}{1 + R_2^2 - 2R_2\cos(\Theta_2 - 2\theta)}. \tag{13}$$

One central issue regarding the study is to identify all the possible collective states either stationary or nonstationary, and reveal various bifurcations as the change of the coupling parameter λ and σ, provided that the initial symmetric distribution has the form of Poisson kernels.

The Riccati equation (12) describes the collective symmetric dynamics of Eq. (2) in terms of the second order parameter r_2, and it can be straightforwardly rewritten in cartesian coordinates $r_2 = x + iy$ as

$$\dot{x} = -2(\omega + \sigma \cdot y - \lambda y)y + \lambda(1 - x^2 - y^2), \tag{14}$$

$$\dot{y} = 2(\omega + \sigma \cdot y - \lambda y)x. \tag{15}$$

In the phase space of the second-order parameter, the natural boundary is $x^2 + y^2 = 1$, a fixed point is determined by the intersection of nullclines $\dot{x} = 0$ and $\dot{y} = 0$ within the boundary. One recalls that the first point is $y_{01} = \omega/(\lambda - \sigma)$ and $x_{01}^2 + y_{01}^2 \equiv 1$, which is on the unit circle and defined as the synchrony state, and the synchrony state exists when $|\lambda - \sigma| \geq \omega$. Additionally, the linearization Jacobian matrix of the synchrony state has two eigenvalues

$\delta_1 = -2\lambda x_{01}$ and $\delta_2 = -2(\lambda - \sigma)x_{01}$, which determines the stability of the synchrony state in the existence regimes. Once again, the same strategy such as the existence and the stability analysis can be actually adopted for the second fixed point $x_{02} = 0$, $y_{02} = (\omega \pm \sqrt{\omega^2 - \lambda(\lambda - 2\sigma)})/(\lambda - 2\sigma)$, which is on the y axis and termed as the splay state[32]. The Jacobian matrix of the second point has two purely imaginary eigenvalues, which shows that the splay state is neutrally stable to perturbations and is a center in the Ott-Antonsen manifold.

Figure 1 presents the phase diagram that summarizes the results of our analysis of Eqs (14) and (15), and we find that there are four different dynamical regimes, i.e., the double-center regime I, the single-center regime II, the center-synchrony coexistence regime III and the synchrony regime IV, respectively. In addition, various bifurcations and transitions among these states are illustrated when the parameters are adjusted to pass through the boundary curves. There are two kinds of routes to synchrony, for instance, when we start from II to IV (arrow 1 in the Fig. 1), the transition to synchrony is a first-order phase transition with hysteresis because of the coexistence regime III. However, when we turn to the second route (arrow 2 in the Fig. 1) the transition is discontinuous and is absent of hysteresis.

The above analysis reveals the low-dimensional collective behaviors of symmetric dynamics, where the bifurcations and transitions among various states are presented. Actually, all the results are within the framework of the Ott-Antonsen invariant manifold including the linear perturbation of the fixed points. In the following, we perform a thorough linear stability analysis of the stationary symmetric distribution in terms of the self-consistent theory[33], where all the boundary curves could be obtained analytically in an alternative way. As it will appear momentarily, when we impose a general perturbation for the steady states, the analytical predictions above are still valid. Meanwhile, the eigenvalues of the steady states keep the same form above and the splay state turns out to be neutrally stable in all directions.

A convenient way of solving the symmetric dynamics is to make the change of variable $\varphi = 2\theta$, which yields a new dynamical equation

$$\dot{\varphi}_i = 2\omega - 2\lambda \sin\varphi_i + \frac{2\sigma}{N}\sum_{j=1}^{N} \sin\varphi_j, \quad i = 1, \cdots, N. \tag{16}$$

Eq. (16) has the form of dynamical equations of over damped linear Josephson junction arrays. It is obvious that the distribution of φ is equivalent to the ρ_s in Eq. (13). The synchrony state corresponds to a spatially homogeneous fixed point of Eq. (16) defined as $\dot{\varphi}_i = 0$, for all the i and $\varphi_1 = \varphi_2 = \cdots = \varphi_N = \varphi_0$ which is the simplest attractor. Therefore, this phase leads to a solution of equation

$$\omega - (\lambda - \sigma)\sin\varphi_0 = 0. \tag{17}$$

In this case $\sin\varphi_0 = \omega/(\lambda - \sigma)$, and the Jacobian matrix of Eq. (16) is a circulant matrix[23,33] with two kinds of eigenvalues. The first one is

$$\delta_1 = -2(\lambda - \sigma)\cos\varphi_0, \tag{18}$$

which corresponds to a spatial homogeneous fluctuation, and the other $N-1$ eigenvalues are

$$\delta_2 = -2\lambda\cos\varphi_0, \tag{19}$$

which have $(N-1)$-fold degeneracy that correspond to inhomogeneous fluctuations. Incidentally, one notes that $x_{01} \equiv \cos\varphi_0$, $y_{01} \equiv \sin\varphi_0$, this result is consistent with a basic fact that the synchrony state is contained in the Ott-Antonsen manifold. Numerical experiment shows that the basin of attraction of the synchrony state in regime IV is global.

Another scenario is the stationary distribution where the phase φ is smoothly distributed over $[0, 2\pi]$, and from Eq. (16) one observes that the general form of such a stationary distribution is

$$\rho_s(\varphi) = \frac{C}{\varpi - 2\lambda\sin\varphi}, \tag{20}$$

where ϖ is the effective frequency, which can be determined self-consistently from the equation

$$\varpi = 2\omega + 2\sigma\int_0^{2\pi} d\varphi \frac{C\cdot\sin\varphi}{\varpi - 2\lambda\sin\varphi}. \tag{21}$$

C is the normalization constant as $C = \pm\sqrt{\varpi^2 - 4\lambda^2}/2\pi$, when $\varpi > 0$, C is positive and vice versa. Substituting the expression of C into Eq. (21), we obtain the solution of ϖ,

$$\varpi = \frac{2[\omega(\lambda - \sigma) \pm \sqrt{\sigma^2(\omega^2 - \lambda^2 + 2\lambda\sigma)}]}{\lambda - 2\sigma}. \tag{22}$$

It should be emphasized that the stationary distribution $\rho_s(\varphi)$ corresponds to the splay state in the invariant manifold above, because the distribution Eq. (20) has the form of Possion kernels, and

$$\langle\sin\ \varphi\rangle = \int_0^{2\pi} \frac{C\cdot\sin\varphi}{\varpi - 2\lambda\sin\varphi} d\varphi = y_{02}, \tag{23}$$

and

$$\langle \cos\ \varphi\rangle = \int_0^{2\pi} \frac{C\cdot\ \cos\varphi}{\varpi - 2\lambda\ \sin\varphi} d\varphi = 0 \equiv x_{02}. \tag{24}$$

The perturbation of the continuity equation for the stationary symmetric distribution $\rho_s(\varphi)$ is

$$\begin{aligned}\frac{\partial}{\partial t}(\delta\rho) &= \hat{L}\delta\rho(\varphi, t)\\ &= -\frac{\partial}{\partial\varphi}[(\varpi - 2\lambda\ \sin\varphi)\,\delta\rho(\varphi, t)] + \frac{\partial\rho_s}{\partial\varphi}\int_0^{2\pi} d\varphi' 2\sigma\sin\varphi'\,\delta\rho(\varphi', t),\end{aligned} \tag{25}$$

and the eigenvalue equation (25) is convenient to be treated in the function space,

$$\frac{\delta\rho(\varphi, t)}{\rho_s(\varphi)} = \sum_{n=-\infty}^{\infty} a_n(t) e^{2\pi i n G(\varphi)}, \tag{26}$$

where $G(\varphi)$ is the basis function

$$G(\varphi) = \int_0^{\varphi} \rho_s(\varphi')\, d\varphi', \tag{27}$$

and $a_n(t)$ are the expansion coefficients. The stability analysis of the stationary distribution (see in the Supplementary Material) indicates that in regimes I, II and III, all the infinitely many eigenvalues of the operator L are purely imaginary, which implies that the stationary distribution is neutrally stable in all directions, not only confined to the Ott-Antonsen manifold. The evidence of a regime where the stationary distribution is marginally stable is termed as the marginal regime[33] and in which there are no particular attractors that the system converges to. Actually, this highly non-generic property is associated with the time-reversal symmetry that the Eq. (16) exhibits. When we start in the Ott-Antonsen manifold, the trajectory of r_2 is a two-dimensional closed periodic curve (see the insert of Fig. 1), however, when we start with a more general initial condition in the marginal regime, the situation differs substantially as we will see in the following part.

The steady and transient dynamics. In the above analysis, we investigated the symmetric dynamics by using two kinds of ways, both the Ott-Antonsen method and the self-consistency theory. One recalls that when the parameters are in regime IV, the symmetric dynamics converge to the steady state, as a result, the two-synchrony-cluster state emerges, i.e., $\sin 2\theta_0 = \omega/(\lambda - \sigma)$, $\cos 2\theta_0 > 0$. Thus, the complete steady state distribution of phase oscillators is

$$\rho_0(\theta) = \left(\frac{1}{2} + c\right)\delta(\theta - \theta_0) + \left(\frac{1}{2} - c\right)\delta(\theta - \theta_0 - \pi), \quad |c| < \frac{1}{2}. \tag{28}$$

$\rho_0(\theta)$ is comprised of two delta functions denoting two clusters of oscillators at $\theta_0 = 0.5\arcsin\omega/(\lambda - \sigma)$ and $\theta_0 + \pi$. Correspondingly, the phase oscillators settle to one of the two stable equilibria, while the unstable equilibria $\pi/2 - \theta_0$ and $3\pi/2 - \theta_0$ serve as the boundaries for the basin of attraction. Therefore, the degree of asymmetry $|r_1|$ is

$$|r_1| = |2c(\cos\theta_0 + i\ \sin\theta_0)| = 2|c|, \tag{29}$$

which depends on the free parameter c and could be determined approximatively from initial condition. Note that $1/2 - c$ is just the fraction of oscillators in the locked phase $\theta_0 + \pi$, namely,

$$c = \frac{1}{2} - \int_{\frac{\pi}{2} - \theta_0}^{\frac{3\pi}{2} - \theta_0} \rho(\theta, t_0)\, d\theta + \varepsilon, \tag{30}$$

where $\rho(\theta, t_0)$ is the initial density, ε is the error caused by the Arnold diffusion. Theoretically, when the initial phase is in the one-dimensional invariant manifold $\theta_1 = \theta_2 = \cdots = \theta_N$ the evolution of phase $\theta(t)$ for all oscillators can never pass through two saddle points $\pi/2 - \theta_0$ and $3\pi/2 - \theta_0$ which means $\epsilon = 0$. However, for the more general initial conditions, some oscillators that are in the neighborhood of two unstable equilibrium states can bypass the saddle points (Fig. 2(b) illustrates schematically the mechanism in the low-dimensional phase space where $N = 3$) and therefore ε is non-negligible. Figure 2(a) presents the numerical simulation when we choose $\theta_0 = \pi/6$ and $\rho(\theta, t_0) = (1 + \cos\theta)/2\pi$, it is clear that the initial phases in the gray area eventually bypass the saddle points (the pink hollow circle in the horizontal axis). This interesting phenomenon can be heuristically understood as follows, those oscillators in the gray area tend to choose a relatively near equilibrium state to settle in the high- dimensional phase space, while this is forbidden in the one-dimensional invariant manifold.

When the symmetric dynamics r_2 approaches the steady state, then the $|r_1|$ dynamics reaches the steady state quickly. However, in a large marginal regime of the phase diagram Fig. 1, the dynamics of r_2 can never converge to an attractor, and the motion of r_2 is time-dependent. To capture the dynamical features of r_1, we can solve the partial differential equation (PDE) (5)

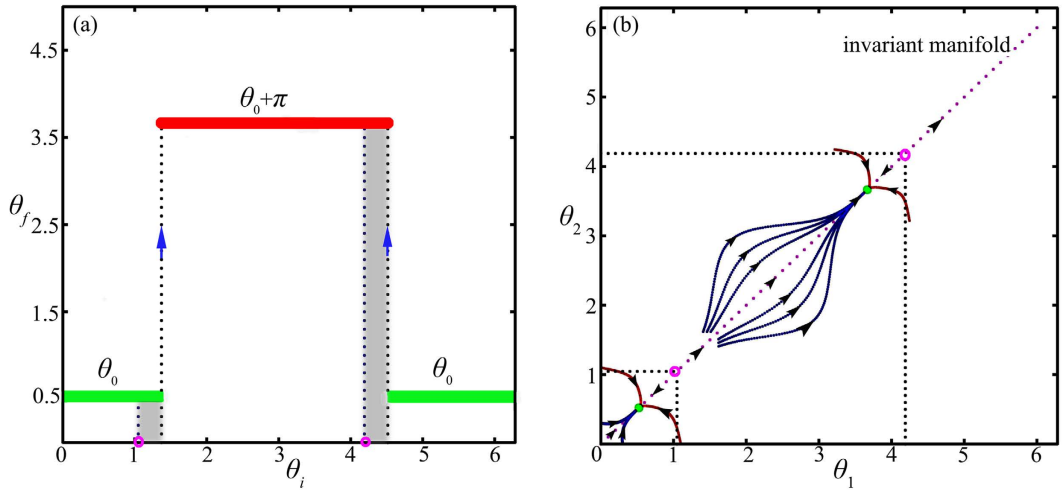

Figure 2. (**a**) The initial phase θ_i vs the final phase θ_f when we choose the initial phase distribution $\rho(\theta, t_0) = (1+\cos\theta)/2\pi$ and the number of oscillator is $N = 10000$ in the simulation, when the initial phase is in the gray area, these oscillators will bypass the saddle points (the pink hollow circle in the horizontal axis) which leads to $\varepsilon \neq 0$. (**b**) The diagram of the Arnold diffusion mechanism in the same parameter with $N = 3$ in terms of the phase space of θ_1 and θ_2. For some particular trajectory, such as the red line, the oscillator will bypass the saddle point in the invariant manifold.

$$\frac{\partial \rho}{\partial t} + (\omega - \lambda \sin 2\theta + \sigma \cdot \mathrm{Im}(r_2))\frac{\partial \rho}{\partial \theta} = \lambda \cos 2\theta \cdot \rho, \tag{31}$$

in terms of the characteristics method. When we start in the characteristic curve $\theta(t, t_0)$, the distribution function will be $\rho(\theta, t) \equiv \rho(\theta(t, t_0), t)$ and the PDE becomes the ODEs. The characteristic equations are

$$\dot{\rho} = 2\lambda \cos 2\theta \cdot \rho, \tag{32}$$

$$\dot{\theta} = \omega - \lambda \sin 2\theta + \sigma \cdot \mathrm{Im}(r_2). \tag{33}$$

When the symmetric dynamics are in the Ott-Antonsen invariant manifold, the motion of r_2 is governed by Eq. (12). Generally, Eqs (32) and (33) are difficult to solve analytically, while for some particular situations e.g., the orbit of r_2 is near to the center point, the fluctuation of r_2 is small enough reflecting that $\mathrm{Im}(r_2)$ is approximately a constant. Then the expression for the characteristic curves $\theta(t, t_0)$ starting at the initial phase θ_0 yields

$$\theta(t, t_0) = \arctan \times \left\{ \frac{\lambda + \sqrt{(\omega + \sigma\ \mathrm{Im}(r_2))^2 - \lambda^2} \cdot \tan[\sqrt{(\omega + \sigma\ \mathrm{Im}(r_2))^2 - \lambda^2}(\theta_0 + t)]}{\omega + \sigma \cdot \mathrm{Im}(r_2)} \right\}, \tag{34}$$

and the distribution along the characteristic equations is

$$\begin{aligned} \rho(t) &= \rho_0 \exp\left[\int_{t_0}^{t} 2\lambda \cos 2\theta(t', t_0)\, dt'\right] \\ &= \rho_0 \exp\left[\int_{\theta_0}^{\theta(t)} 2\lambda \cos 2\theta(t', t_0) \cdot \frac{dt'}{d\theta} \cdot d\theta\right] \\ &= \frac{\rho_0(\omega - \lambda \sin 2\theta_0 + \sigma \cdot \mathrm{Im}(r_{20}))}{\omega - \lambda \sin 2\theta(t, t_0) + \sigma \cdot \mathrm{Im}(r_2)}, \end{aligned} \tag{35}$$

where ρ_0 is the initial value of the distribution function, r_{20} is the initial value of r_2. Theoretically, the general form of the density function $\rho(\theta, t)$ could be determined by substituting the inverse solution $\theta_0(\theta(t))$ Eq. (34) into Eq. (35), and the generalized order parameters could also be obtained through the integral Eq. (6). Due to the multivalue feature of the anti-trigonometric function Eq. (34), it is convenient to calculate the first-order parameter r_1 via the integral

$$r_1(t) = \int_{-\pi}^{\pi} \rho(t) e^{i\theta(t, t_0)} \cdot \frac{\partial \theta(t, t_0)}{\partial \theta_0} \cdot d\theta_0. \tag{36}$$

From Eq. (36) and Fig. 3(a), we find that $|r_1(t)|$ oscillates regularly with a period

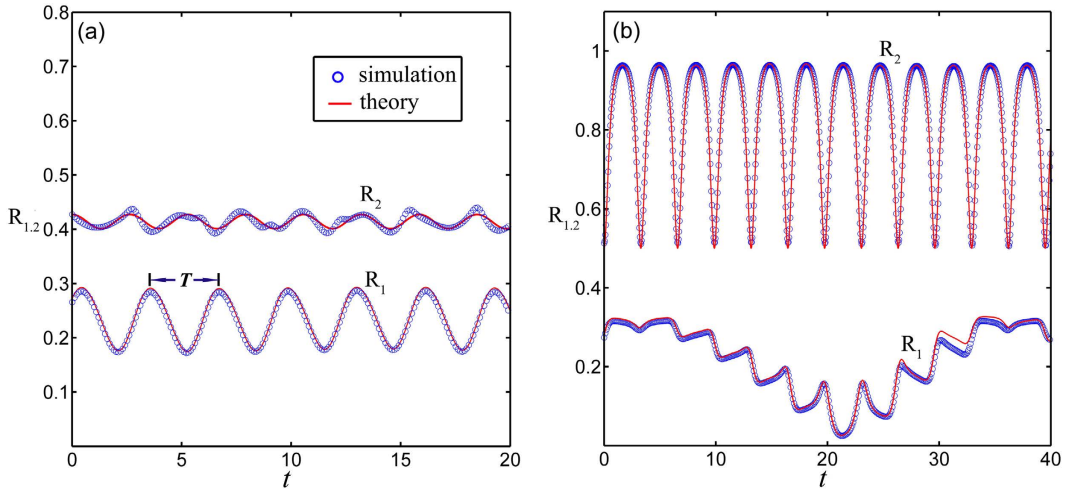

Figure 3. Transient dynamics of R_1 and R_2. (**a**) When the amplitude of R_2 is small, R_1 oscillates regularly with a period T, $\sigma = 1.0$, $\lambda = 1.0$, $\mathrm{Re}(r_{20}) = 0$, and $\mathrm{Im}(r_{20}) = 0.427$. (**b**) When the amplitude of R_2 is large, R_1 oscillates irregularly, $\sigma = 1.0$, $\lambda = 1.4$, $\mathrm{Re}(r_{20}) = 0$, and $\mathrm{Im}(r_{20}) = -0.5$. In the numerical simulation we choose the initial phase distribution $\rho(\theta, t_0) = \rho_s(2\theta, t_0)(1 + 0.5\cos(\theta))$ and $N = 10000$, the line is calculated by the characteristic theory and the circle is the numerical simulation.

$$T = \frac{\pi}{\sqrt{(\omega + \sigma \cdot \mathrm{Im}(r_2))^2 - \lambda^2}}. \tag{37}$$

When the fluctuation of r_2 is considerably large, the time dependence of r_1 is irregular as shown in Fig. 3(b).

The discussion of the symmetric dynamics Eq. (16) exhibits a two-dimensional Ott-Antonsen manifold proving that the initial symmetric distribution takes the form of Possion kernels Eq. (13). In fact, the significant works point out that the evolution equations for the form of Eq. (16) are generated by the action of the Möbius group[34,35]

$$e^{i\varphi_j(t)} = \frac{e^{i\psi}e^{i\phi_j} + \alpha}{1 + \alpha^* e^{i\psi} \cdot e^{i\phi_j}}, \tag{38}$$

α is a complex variable, ψ is real, and ϕ_j is the motion constant. The group action partition the N-dimensional state space into a three-dimensional invariant manifold, and the three parameters $\mathrm{Re}(\alpha)$, $\mathrm{Im}(\alpha)$, ψ are governed by the following equations

$$\dot{\mathrm{R}}e(\alpha) = -2(\omega + \sigma \cdot \mathrm{Im}(r_2) - \lambda \cdot \mathrm{Im}(\alpha)) \cdot \mathrm{Im}(\alpha) + \lambda(1 - |\alpha|^2), \tag{39}$$

$$\dot{\mathrm{I}}m(\alpha) = 2(\omega + \sigma \cdot \mathrm{Im}(r_2) - \lambda \cdot \mathrm{Im}(\alpha)) \cdot \mathrm{Re}(\alpha), \tag{40}$$

$$\dot{\psi} = 2(\omega + \sigma \cdot \mathrm{Im}(r_2) - \lambda \cdot \mathrm{Im}(\alpha)). \tag{41}$$

When the motion constant takes a general distribution, the parameter r_2 can be written in terms of α and ψ as[34]

$$r_2 = \alpha + (|\alpha|^2 - 1)\sum_{n=1}^{\infty}(-1)^n c_n^* e^{in\psi}(\alpha^*)^{n-1}, \tag{42}$$

c_n is the n-th Fourier expansion coefficient of the distribution of motion constants. For the simple case, where the distribution is uniform on $[0, 2\pi]$, $c_n \equiv 0$ for all the n, $r_2 \equiv \alpha$, and α decouples from ψ. This implies that the three-dimensional state space has a two-dimensional invariant submanifold which is indeed the Ott-Antonsen manifold. However, in the more typical case where α and ψ are interdependent, the three-dimensional equation can exhibit non-general dynamical features in the marginal regime.

In Fig. 4(a), we use Poincare section at $\psi(\mathrm{mod}\ 2\pi) = 0$ to sort out the structure of state space, where the parameters are chosen in regime II of Fig. 1 ($\lambda = 1.5$ and $\sigma = 2.0$), and the motion constant has a distribution $(1 + \sin\phi)/2\pi$. In the Poincare section, quasiperiodic trajectories appear as closed curves or island chains, periodic trajectories appear as fixed points or period-p points of integer period, and chaotic trajectories fill the remaining regimes of the unit disk. The picture of the phase portraits in the marginal regime resembles the phenomenon of Hamiltonian chaos in the classical integrable system, and the appearance of the quasi-Hamiltonian properties originates form the time reversibility symmetry under the transformation $t \to -t$, $\psi \to -\psi$, $x \to -x$, that the evolution equations are invariant. When we choose the initial value in the chaos regime, $\alpha(0) = 0.5 + i$ 0.5, $\psi(0) = 0.0$, the three Lyapunov exponents are $\lambda_1 = -0.266$, $\lambda_2 = 0$, $\lambda_3 = 0.227$, respectively. As a result, the

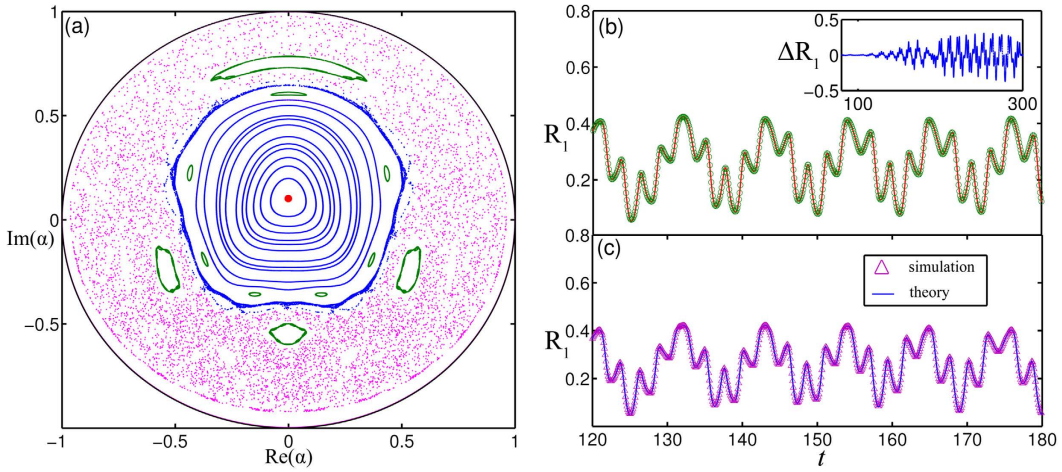

Figure 4. (**a**) Poincare section of Eqs (39)~(41) at $\psi(\mathrm{mod}\ 2\pi) = 0$, quasiperiodic trajectories appear as closed curves or island chains, periodic trajectories appear as fixed points or period-p points of integer period, and chaotic trajectories fill the remaining region of the unit disk, where $\omega = 1.0$, $\lambda = 1.5$, $\sigma = 2.0$. (**b**) R_1 vs t in the chaos regime with $\alpha(0) = 0.5 + i\,0.5$ and $\psi(0) = 0.0$. (**c**) R_1 vs t with adjacent parameter value $\delta\alpha(0) = 0.001$, $\delta\psi(0) = 0$. The insert is the difference of R_1 vs t where we can see that the bias of the order parameter with neighboring parameters will be significant in the long time. In the simulation we choose $N = 100000$ and the initial phase distribution $\rho(\theta, t_0) = \rho_s(2\theta, t_0)\,(1 + 0.5\cos(\theta))$, where $\rho_s(2\theta, t_0)$ is determined by Eq. (38), the line is determined in terms of the the characteristic theory and the circle and triangle are calculated by the numerical simulation.

evolution of order parameters r_2 and r_1 is also chaotic which are sensitive to initial values. Figure 4(b,c) depict the evolution of $R_1(t)$ with two adjacent parameter values where $\delta\alpha(0) = 0.001$, $\delta\psi(0) = 0$. It is clear that the bias of order parameter with neighboring parameters (the insert in the Fig. 4(b)) will be significant in the long time and the characteristic curve and numerical simulation are consistent with each other well.

Discussion

To summarize, we investigated the collective dynamics of globally coupled identical phase oscillators when second harmonics dominate the coupling, and solutions can be decomposed into symmetric and antisymmetric parts independently. Theoretically, the Ott-Antonsen method, the linear stability analysis, and the characteristic method have been respectively carried out to obtain analytical insights. Together with numerical simulations, our study presented the following main results. First, we obtained the low-dimensional description of the symmetric dynamics, and various regimes are predicted in the phase diagram, including the double-center, the single-center, the center-synchrony coexistence, and the synchrony regime. Second, all the steady states and the boundary curves have been obtained analytically both in terms of the Ott-Antonsen ansatz and the linear stability analysis. Third, we proved that in the marginal regime, the stationary symmetry distribution is only neutrally stable, where all the infinitely many eigenvalues are purely imaginary. Finally, the characteristic method has been adopted to obtain the transient dynamics r_1 whose evolution strongly depends on the initial values. Furthermore, for the general case of initial condition, the symmetry dynamics are governed by the Möbius transformation and numerical experiment suggested that three-dimensional invariant manifolds contain neutrally stable chaos in the marginal regime. This work provided a complete framework to deal with the high-order coupling phase oscillators model, and the obtained results will enhance our understandings of the dynamical properties of coupled phase oscillator systems with more higher-order harmonic coupling terms.

References

1. Pikovsky, A., Rosenblum, M. & Kurths, J. *Synchronization*: *a universal concept in nonlinear sciences*. pp. 279–296 (Cambridge University Press, Cambridge, England, 2001).
2. Buck, J. Synchronous rhythmic flashing of fireflies. II. *The Quarterly Review of Biology* **63,** 265–289 (1988).
3. Georges, B., Grollier, J., Cros, V. & Fert, A. Impact of the electrical connection of spin transfer nano-oscillators on their synchronization: an analytical study. *Appl. Phys. Lett.* **92,** 232504 (2008).
4. Kiss, I. Z., Zhai, Y. & Hudson, J. L. Emerging coherence in a population of chemical oscillators. *Science* **296,** 1676–1678 (2002).
5. Eckhardt, B., Ott, E., Strogatz, S. H., Abrams, D. M. & McRobie, A. Modeling walker synchronization on the Millennium Bridge. *Phys. Rev. E* **75,** 021110 (2007).
6. Néda, Z., Ravasz, E., Vicsek, T., Brechet, Y. & Barabási, A. L. Physics of the rhythmic applause. *Phys. Rev. E* **61,** 6987–6992 (2000).
7. Kuramoto, Y. *Chemical oscillations*, *waves*, *and turbulence*. pp. 75–76 (Springer, Berlin, 1984).
8. Strogatz, S. H. From Kuramoto to Crawford: exploring the onset of synchronization in populations of coupled oscillators. *Physica D* **143,** 1–20 (2000).
9. Acebrón, J. A., Bonilla, L. L., Vicente, C. J. P., Ritort, F. & Spigler, R. The Kuramoto model: A simple paradigm for synchronization phenomena. *Rev. Mod. Phys.* **77,** 137–185 (2005).
10. Arenas, A., Diaz-Guilera, A., Kurths, J., Moreno, Y. & Zhou., C. Synchronization in complex networks. *Phys. Rep.* **469,** 93–153 (2008).

11. Rodrigues, F. A., Peron, T. K. D. M., Ji, P. & Kurths, J. The Kuramoto model in complex networks. *Phys. Rep.* **610,** 1–98 (2016).
12. Skardal, P. S., Ott, E. & Restrepo, J. G. Cluster synchrony in systems of coupled phase oscillators with higher-order coupling. *Phys. Rev. E* **84,** 036208 (2011).
13. Komarov, M. & Pikovsky, A. Multiplicity of singular synchronous states in the Kuramoto model of coupled oscillators. *Phys. Rev. Lett.* **111,** 204101 (2013).
14. Komarov, M. & Pikovsky, A. The Kuramoto model of coupled oscillators with a bi-harmonic coupling function. *Physica D* **289,** 18–31 (2014).
15. Li, K., Ma, S., Li, H. & Yang, J. Transition to synchronization in a Kuramoto model with the first- and second-order interaction terms. *Phys. Rev. E* **89,** 032917 (2014).
16. Czolczynski, K., Perlikowski, P., Stefanski, A. & Kapitaniak, T. Synchronization of the self-excited pendula suspendedon the vertically displacing beam. *Commun. Nonlinear Sci. Numer. Simul.* **18,** 386–400 (2013).
17. Zhang, J., Yuan, Z. & Zhou, T. Synchronization and clustering of synthetic genetic networks: a role for cis-regulatory modules. *Phys. Rev. E* **79,** 041903 (2009).
18. Kiss, I. Z., Zhai, Y. & Hudson, J. L. Predicting mutual entrainment of oscillators with experiment-based phase models. *Phys. Rev. Lett.* **94,** 248301 (2005).
19. Goldobin, E., Koelle, D., Kleiner, R. & Mints, R. G. Josephson junction with a magnetic-field tunable ground state. *Phys. Rev. Lett.* **107,** 227001 (2011).
20. Goldobin, E., Kleiner, R., Koelle, D. & Mints, R. G. Phase retrapping in a pointlike φ Josephson junction: the butterfly effect. *Phys. Rev. Lett.* **111,** 057004 (2013).
21. Gómez-Gardeñes, J., Gómez, S., Arenas, A. & Moreno, Y. Explosive synchronization transitions in scale-free networks. *Phys. Rev. Lett.* **106,** 128701 (2011).
22. Zou, Y., Pereira, T., Small, M., Liu, Z. & Kurths, J. Basin of attraction determines hysteresis in explosive synchronization. *Phys. Rev. Lett.* **112,** 114102 (2014).
23. Xu, C., Gao, J., Sun, Y., Huang, X. & Zheng, Z. Explosive or Continuous: Incoherent state determines the route to synchronization. *Sci. Rep.* **5,** 12039 (2015).
24. Coutinho, B. C., Goltsev, A. V., Dorogovtsev, S. N. & Mendes, J. F. F. Kuramoto model with frequency-degree correlations on complex networks. *Phys. Rev. E* **87,** 032106 (2013).
25. Kazanovich, Y. & Borisyuk, R. Synchronization in oscillator systems with a central element and phase shifts. *Progress of Theoretical Physics* **110,** 1047–1057 (2003).
26. Burylko, O., Kazanovich, Y. & Borisyuk, R. Bifurcations in phase oscillator networks with a central element. *Physica D* **241,** 1072–1089 (2011).
27. Kazanovich, Y., Burylko, O. & Borisyuk, R. Competition for synchronization in a phase oscillator system. *Physica D* **261,** 114–124 (2013).
28. Vlasov, V., Zou, Y. & Pereira, T. Explosive synchronization is discontinuous. *Phys. Rev. E* **92,** 012904 (2015).
29. Vlasov, V., Pikovsky, A. & Macau, E. E. N. Star-type oscillatory networks with generic Kuramoto-type coupling: A model for "Japanese drums synchrony". *Chaos* **25,** 123120 (2015).
30. Ott, E. & Antonsen, T. M. Low dimensional behavior of large systems of globally coupled oscillators. *Chaos* **18,** 037113 (2008).
31. Ott, E. & Antonsen, T. M. Long time evolution of phase oscillator systems. *Chaos* **19,** 023117 (2009).
32. Watanabe, S. & Strogatz, S. H. Constants of motion for superconducting Josephson arrays. *Physica D* **74,** 197–253 (1994).
33. Golomb, D., Hansel, D., Shraiman, B. & Sompolinsky, H. Clustering in globally coupled phase oscillators. *Phys. Rev. A* **45,** 3516–3530 (1991).
34. Marvel, S. A., Mirollo, R. E. & Strogatz, S. H. Identical phase oscillators with global sinusoidal coupling evolve by Möbius group action. *Chaos* **19,** 043104 (2009).
35. Marvel, S. A. & Strogatz, S. H. Invariant submanifold for series arrays of Josephson junctions. *Chaos* **19,** 013132 (2009).

Acknowledgements

This work is partially supported by the NSFC grants Nos 11075016, 11475022, and the Scientific Research Funds of Huaqiao University.

Author Contributions

C.X., H.X., J.G. and Z.Z. designed the research; C.X., H.X. and J.G. performed numerical simulations and theoretical analysis; C.X. and Z.Z. wrote the paper. All authors reviewed and approved the manuscript.

Additional Information

Supplementary information accompanies this paper at http://www.nature.com/srep

Competing financial interests: The authors declare no competing financial interests.

How to cite this article: Xu, C. *et al.* Collective dynamics of identical phase oscillators with high-order coupling. *Sci. Rep.* **6**, 31133; doi: 10.1038/srep31133 (2016).